Journal of Materials & Environmental Sustainability Research (2022), 2(2): 1-10
p-ISSN: 2811-1338; e-ISSN: 2811-132X
DOI: https://doi.org/10.55455/jmesr.2022.004

Original Research Paper

Effect of polymer concentrations on pores mechanism in electrospun fibre

Samson O. Alayande [1]*, Oluseyi A. Adeyemi [2], Oyesolape B. Akinsipo [3], Joshua N. Edokpayi [4], Gabriel O. Oladipo [5], Titus A.M. Msagati [6]

[1] Department of Physical Sciences, First Technical University, Oyo State, Nigeria
[2] Department of Mechanical and Mechatronic Engineering, First Technical University, Oyo State, Nigeria
[3] Department of Chemical Sciences, Tai Solarin University of Education, Ogun State, Nigeria
[4] Department of Hydrology and Water Resources, University of Venda, Thohoyandou 0950, South Africa
[5] Department of Science Laboratory Technology, D.S. Adegbenro ICT Polytechnic, Ogun State, Nigeria
[6] Nanotechnology and Water Sustainability, University of South Africa, Florida, South Africa
*Corresponding author: Samson O. Alayande (samson.alayande@tech-u.edu.ng)

Received: January 11, 2022; Revised: April 16, 2022; Accepted: April 25, 2022; Published: May 11, 2022

Handling Editor: Ubong J. Etim

Abstract:
Advanced material science has resulted in materials with atomic-scale dimensions whose tremendous application includes filtration, drug delivery, membrane, sensor, and encapsulation. Nanoporous fibre has been formed using temperature-induced phase separation (TIPS) and vapour-induced phase separation (VIPS) mechanism, but polymer concentration has been underestimated in the electrospinning parameter. This work aims at showcasing the effect of electrospinning parameters including polymer concentration and resultant phases on pore formation on fibre. Pore formation in electrospun fibre was carried out by electrospinning expanded polystyrene (EPS). The surface morphology of the resulting nanoporous fibre was characterized with Scanning Electron Microscope (SEM) while the pore distribution was analyzed with a BET (Brunauer, Emmet, Teller) micromeritics analyzer. From the result, an increased concentration of polymer from 10 % decreased bead population to zero, meanwhile, bombardment with high electrostatic power resulted in beaded fibres at 10% and 15% w/v. Further increase in EPS concentration resulted in beadless fibres and electrospun 20% EPS fibre at 8.5 kV resulted in porous fibre with meso, micro and macropores. At 11.5 kV, pore dimension in fibre reduced with predominant pore width less than 100 nm. An increased voltage to 13.5 kV resulted in morphologies showing brittled fibre probably due to excess pores formed. Conclusively, polymer concentration moderates variables interaction that resulted in phase separation which controls fibre orientation. Therefore, pore formation does not solely depend on TIPS, VIPS, and breath figures but also polymer concentration.

Keywords: nanofibre; electrolysis; pore orientation; concentration; mechanism

DOI: 10.55455/jmesr.2022.004

1. Introduction

In the last two decades, the multifaceted application of expanded polystyrene (EPS) in roofs and walls of buildings, containers, packaging materials etc. has propelled its massive production. Meanwhile, the lack of suitable disposal facilities and reuse of EPS remains a consequential global issue, instead, its environmental pile-up is increasingly unsettling (Uttaravalli et al. 2020). Annually, polystyrene (PS) occupies 10 wt. % of the total plastic waste produced in the last ten years, while its monomer, styrene is as a toxin capable of causing cancer. Styrene has also been suspected to be toxic to the gastrointestinal tract (GIT) including the respiratory and renal systems. Efforts made to solve its environmental implication returned with deleterious effects such as global warming and the persistence of plastic waste (Hidalgo-Crespo et al. 2022). Therefore, sustainable management and effective utilization of EPS for advanced applications need to be considered as a solution. Different

techniques including thermal and catalytic degradation have been used in the conversion of EPS waste into either solid or liquid fuels but these techniques are cost-effective (Aljabri et al. 2017). The electrospinning technique is a flexible, versatile and simple way of producing micro and nanofibrous scaffolds which may/may not contain ordered or disordered hierarchical porosity (Aziz et al. 2019; de Farias et al. 2022; Pierini et al. 2017). Several works of literature have described the basic principle of electrospinning in reviews and text (Rudisill et al. 2012; Alayande et al., 2016a; Alayande et al. 2016b; Alayande et al. 2017; Mirjalili & Zohoori, 2016; Xue et al. 2019; Jalali et al. 2021;). For porous fibre, a notable property is the formation of the pores. Based on porosity, porous electrospun fibres have found application in filtration (Alayande et al., 2017; Jalali et al. 2021; Mirjalili & Zohoori, 2016; Xie et al., 2020), drug delivery (Alayande et al. 2017; Xue et al. 2019) and membrane science (Rudisill et al., 2012; Alayande et al., 2016a; Alayande et al. 2016b; Mirjalili & Zohoori 2016;), catalysis (Ding & Yu 2014; Alayande et al. 2017; Xue et al. 2019) encapsulation (Alayande et al. 2017; Xue et al. 2019) etc. Pores can either be inter or intra fibre in electrospun fibres. The inter-fibre pores are formed with controllable width and shape in a non-woven mesh of the fibres (Aziz et al. 2019) while intra-fibre pores exist as a result of polymer solidification during the electrospinning experiment, rather within the fibre inner matrix.

Pore formation involves polymer phase separation and post-treatment methods. Post-treatment methods are associated with solvent extraction; calcination and templating. In the case of the electrospinning process, post-treatment methods usually require additional steps, making the route complex and unattractive (Lu et al., 2011; Zhang et al., 2022). On the other hand, phase separation is a simple and single step, it involves solvent, relative humidity, vapour pressure, temperature, flow rate and collection distance (Alayande 2012; Yadav et al. 2018; ŞİMŞEK, 2019; Szewczyk & Stachewicz 2020; Knapczyk-Korczak et al. 2021). There are two common mechanisms relevant to phase separation for pore formation: thermally induced phase separation (TIPS) (Aziz et al. 2019; Szewczyk & Stachewicz 2020) and vapour induced -phase separation (VIPS) (Alayande et al. 2016a; Aziz et al. 2019; Szewczyk & Stachowicz 2020). TIPS involves liquid jet migration through the bimodal curve into a metastable state where separation takes place into solvent-rich and polymer-rich phases. In electrospinning, solvents escape from the matrix through evaporation leaving behind a solid matrix predominantly dominated by the polymer. Rapid evaporation of the solvent can result in a reduction in temperature, which creates voids on the matrix surface. These voids are known as pores. On the other hand, VIPS explained the role of non-solvent in phase separation. During electrospinning, non-solvent from the vapour phase penetrates polymer solution, precipitating polymer into the solid matrix. This evolves non-solvent evaporation resulting in voids, hereby creating porous regions (Alayande 2012; Aziz et al. 2019; Knapczyk-Korczak et al. 2021).

The previous assumption that TIPS played a crucial role during pore formation in electrospun fibre (Alayande, 2012; Alayande et al. 2016c) was recently invalidated (Aziz et al. 2019). Lu and Younan (Aziz et al. 2019) established the essential role of non-solvent (water vapour) and humidity in the production of polystyrene fibres with porous structures. These factors established VIPS as an indispensable model for pores formation in electrospun fibres. A congest factor still underestimated is polymer concentration. To the best of our knowledge, there is no report relating electrospinning parameters: polymer concentration, resultant phases (polymer and solvent rich phases formed during elongation process) and pore formation on fibre. Such knowledge is necessary for porous membrane development where pore parameters (adhesion, migration, proliferation and ingress properties) are important to ascertain potential application in tissue engineering, energy, catalysis, etc. Also, the use of secondary electron (SE) and backscattered electron (BSE) detectors in the electron microscope for surface morphology examination of porous materials was validated.

Given this, expanded polystyrene (EPS) was used in place of polystyrene to promote the re-use of EPS in membrane processes. The motivation for this study was based on developing viable re-use for EPS besides solid-phase extraction sorbent (Alayande et al. 2016a; SIMHA 1949), petroleum adsorbent (Alayande et al. 2016b; Rudisill et al. 2012) and ultra-low dense material carrier (Aziz et al. 2019). Understanding pore science in the fibre will promote its application in tissue engineering, regenerative medicine and drug delivery.

2. Materials and Methods

2.1 *Preparation of electrospun fibre*

EPS was sourced from packaging material (EPS used for packaging of a computer -product ID 00331-10000-00001-AA595) and was used without further purification. About 10-30% (w/v) EPS was prepared in tetrahydrofuran

(THF) and stirred for 6 hrs. The solution was loaded into a 10 mL syringe connected to a syringe pump with a flow rate of 10 μL/min. The distance between the collector and syringe was set at 20 cm, 8.5-18.5 kV was applied using a direct current power supply (high voltage source (0-40 kV) and deposition was collected on aluminium foil (15 cm x 15 cm). All experiments were carried out at room temperature and relative humidity of 45 ± 2% which was determined by a lab-scale humidifier.

Surface morphology analysis of electrospun fibre: Scanning electron microscope (SEM) micrographs of the fibres were obtained using a TESCAN (USA) model of SEM. Exactly, 1 cm x 1 cm sample was coated with gold for 1 min using a sputtering machine. Images were viewed at an accelerating voltage of 20 kV and further processed using ImageJ software (National Institutes of Health, USA). In this porous material, 20% EPS fibres were comparatively examined using the secondary electron (SE) and backscattering electron (BSE) at various applied voltages.

Pore distribution: Fibres were analyzed with BET micromeritics ASAP 2020 analyzer by Brunauer-Emmett-Teller technique for N_2 gas adsorption-desorption isotherms and pore distribution curves.

3. Results and Discussions

At 10% w/v, essential polymer chain entanglement within the solution is inadequate for the sustenance of continuous formation of a jet during the spinning process, the beaded fibre was obtained. At this concentration, a high concentration of free solvent molecules will congregate to form spherical shapes due to the decreasing surface area per unit mass of the solution. As concentration increases, the bead population reduces to zero (Figure 1 (A1-A3)). This may be due to an increase in solution viscosity, which affects the orientation of polymer in solution and effective hydrodynamic volume. Basically, at a low concentration such as 10% w/v, viscosity and effective hydrodynamic volume may be low, resulting in beads formation during elongation. The electrospinning elongation process involves interaction between solute and solvent. This interaction influences hydrodynamic properties resulting in polymer-rich (solvent deficiency) and deficiency (solvent rich) phases (Haller et al. 2013). Evidence of beads at 15% (w/v) (Fig. 2 (A4-A6)) shows similar behaviour to the previous concentration. However, the reduction of beads population may be due to an increase in concentration. Bombardment with high electrostatic power resulted in beaded fibres for 10% and 15% w/v (Figure 1 (A1-A3) & 2 (A4-A6)), instability in the elongation process during Taylor cone formation may be due to the low concentration which favours solvent rich phase also known as polymer deficiency phase. This may be responsible for the prevalence of beads in the fibres.

It is also worthy to note that at low concentrations, an increase in charge favours the bead population (Shepa et al. 2021; Xue et al. 2017). The polymer solution will aggregate around the electrode when an electric field is applied. On application of positive voltage to the spinneret containing polymer solution, liked polar ions are compelled to aggregate at the surface. This leads to a generation of an electric field by the surface charge, aggregation of ions is then distorted into cone shape known as Taylor cone. Surface tension is suppressed by electrostatic forces when the electric potential of the surface is greater than a critical value. The electrospinning jet can be referred to as a string of charge elements connected by a viscoelastic medium comprising fixed and free ends. Chaotic motion is notable in the free end of the jet which is majorly dependent on the interaction of intrinsic viscosity, surface tension, and electrostatic forces. Intrinsic viscosity and surface tension are related to polymer solution hydrodynamic volume. Theoretically, intrinsic viscosity and surface tension are proportional to the shape of the polymer coil in solution, therefore the amount of solute determines orientation (Haller et al. 2013; Xue et al. 2019). Further increase in EPS concentration resulted in beadless fibres (Figures 3 (A7-A9) & 4 (B1-B3)). The clear change in fibre morphology observed may be due to phase transitions. Concentration can alter the orientation of polymer shape during elongation, therefore, an increase in solute content will lead to an abundance of the polymer in solution, establishing stability during Taylor cone formation.

The porous fibres were observed at 20 and 30% w/v EPS, although previous beaded fibres were porous, the irregular shape of beads makes them undesirable for advanced applications. The common mechanism for pore formation in electrospun fibre is TIPS and VIPS which depend on solvent, temperature, and humidity. While humidity and non-solvent effects favoured solvent rich phase (polymer deficient), an increase or decrease in

polymer concentration results in polymer-rich or deficient phase respectively. Notable pores on the fibre surface may be due to evaporation of volatile solvent resulting in rapid cooling around the environment of the polymer matrix, while penetration of water vapour was disallowed and sheath formation hindered, jet-air separates into phases. At this point, the volatile solvent will have higher vapour pressure than water, thereby saturating the jet-air interphase. Then, water vapour condenses on the polymer matrix resulting from the jet-air interphase, thus creating voids known as pores. Also, pores can be created through charge-charge interactions (Aziz et al. 2019). This interaction is primarily due to the contribution of polymer concentration to positive charges distribution on stretching during Taylor cone formation. Thus, an attraction of condensed water droplets (non-solvent) from the rapid cooling environment occurs. The number of condensed water droplets will be favoured with volatile solvents. The resultant pores (Figure 3 (A7-A9)) have an irregular shape, such orientation is classified as a closed pore. The dimension of pores was calculated using ImageJ software and pore width ranges from less than 2 to 300 nm. In other words, electrospun 20% EPS fibre at 8.5 kV resulted in porous fibre with meso, micro and macropores (Figure 3 (A7)). At 11.5 kV, pore dimension in fibre reduced, predominant pore width was less than 100 nm (Figure 3 (A8)). When the voltage was increased to 13.5 kV, morphologies revealed brittle fibre probably due to excess pores formed. The interconnection of pores could result in breakage as presented in Figure 3 (A9). The pore orientation revealed an irregular shape in the fibre. Each pore had terminal point: again, closed pores were generated. There was no impregnation of pores within the pore which may signify that the formation of pores follows the same mechanism. The pores formed in the fibres did not have a uniform dimension, this can also be classified as disordered pores.

Increasing EPS concentration to 30% (w/v) with an applied voltage of 8.5 kV resulted in porous fibre, pore orientation shows slight alignment (Figure 4 (B1)). These morphologies were similar to that obtained at higher voltage using lower concentration as seen in Figure. 3 (A7-A9), however, pore width was reduced below 250 nm. At 11.5 kV, the surface morphology revealed two distinct phases; porous and non-porous (smooth) (Figure 4 (B2)), while smooth non-porous fibre was obtained at 13.5 kV (Figure. 4 (B3)). Critical examination of Figure. 4 (B2) shows a trace region of smooth morphology at 11.5 kV with no resultant pore. These regions increased with an increase in applied voltages on the fibre. The resultant fibres at 8.75 kV and 11.5 kV have similar pore orientation. Average pore width ranges from 227 nm to 502 nm at 8.75 kV and 11.5 kV, respectively.

Relating the pore orientation of resultant electrospun fibres at 20% and 30% (w/v) EPS electrospun fibre, showed that pore formations were not based on TIPS, VIPS and breath figure only (Alayande et al. 2016c; Aziz et al., 2019). Other parameters such as polymer concentration and electrostatic force (charge effect) also played a prominent role. TIPS and breath figures have been reported as the mechanism responsible for the formation of external pores on electrospun fibres (Alayande et al. 2016c; Aziz et al. 2019; Szewczyk & Stachowicz 2020), these factors are associated with solvent and humidity effects respectively. Both effects might bring about two distinct phases: polymer and solvent phases (Jalali et al. 2021; Xue et al. 2019). These phases determine the orientation of resultant pores on the electrospun fibres. For instance, 20% w/v EPS at 8.5 kV resulted in a disordered pore with irregular pore orientation (Figure 3 (A7)) while the same voltage showed a trend of pore alignment at higher concentration (Figure 4 (B1)). Considering 20 and 30% (w/v) EPS at the same applied voltage, higher polymer concentration in the latter favoured the polymer-rich phase. When polymer concentration increases, the polymer-rich phase will be favoured, leading to a decrease in pore dimension and the tendency for pore alignment. This might be responsible for the difference in pore dimensions and orientations. Polymer rich phase increased simultaneously with electrostatic force (applied voltage) during the electrospinning process, evidenced in micrographs presented in Figures 1 to 4. As electrostatic force increases, polymer solution gains more energy to move faster during jet transportation. This factor favours polymer migration and solvent evaporation from the metallic syringe to the charged electrode (Xue et al. 2017; Sherpa et al. 2021). More charged polymer solution will be obtained on the charged substrate; hence polymer-rich phase will be favoured over the solvent rich phase.

Electrospun fibres, using BSE and SE are shown in Figure 5 (C1-C6), respectively. A clear image of fibres was revealed by both detectors. SEM is a recommended IUPAC analytical tool for the analysis of porous materials. It is used majorly for imaging of surface morphology of the material. Micrographs from SE and BSE resulted in the same morphology, the notable difference might be based on the contrast effect (Figure 5 (C1-C6)). Both detectors revealed porous fibre with non-uniformity in dimension. For the three fibre samples investigated, both SE and BSE images showed clear, visible, multi-irregular shape pores, and the resolution of contrast of SE micrographs

was slightly better than BSE images. These results validate the conventional recommendation of SE or SE+BSE detector for imaging of single and multi-phase samples. Also, a BSE detector can be used for imaging porous materials.

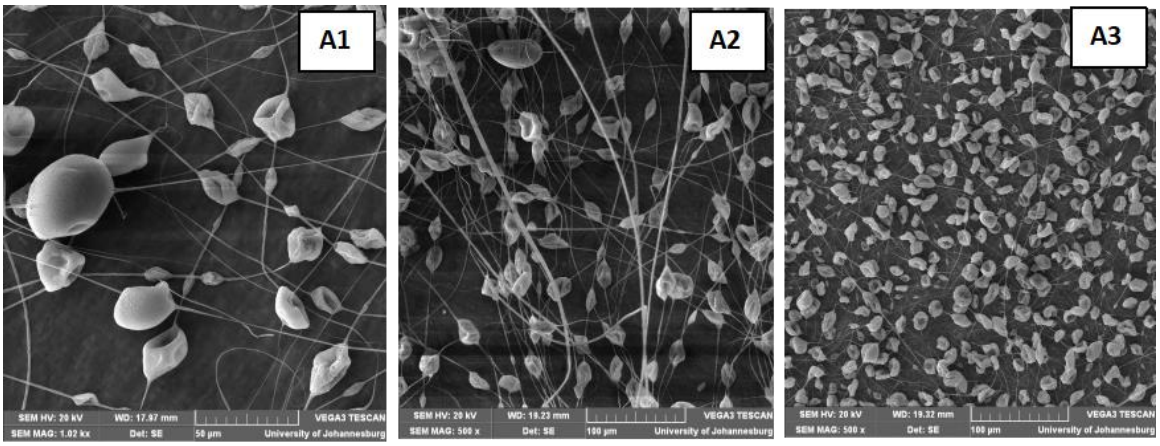

Figure 1: Micrograph of 10% EPS at [A1] 8.5 kV [A2] 11.5 kV [A3] 13.5 kV

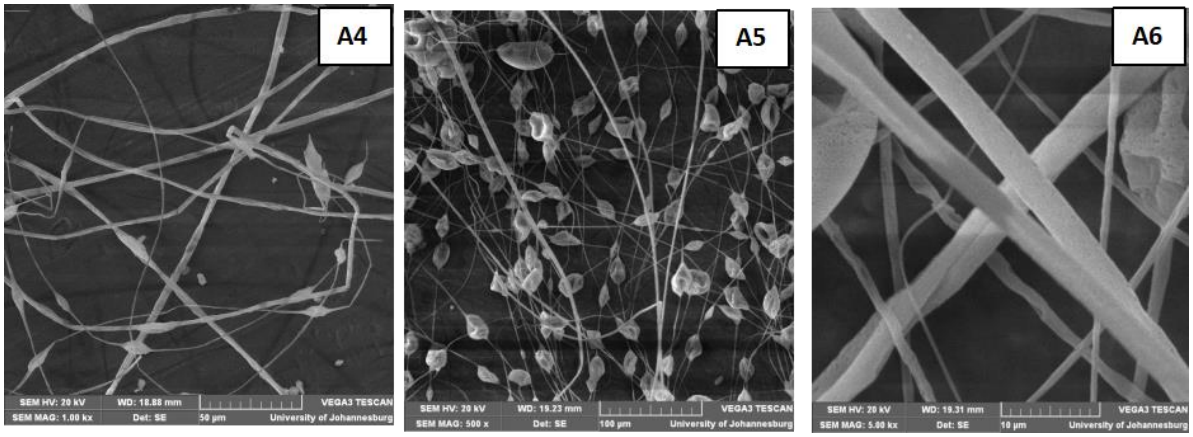

Figure 2: Micrograph of 15% EPS at [A4] 8.5 kV [A5] 11.5 kV [A6] 13.5 kV

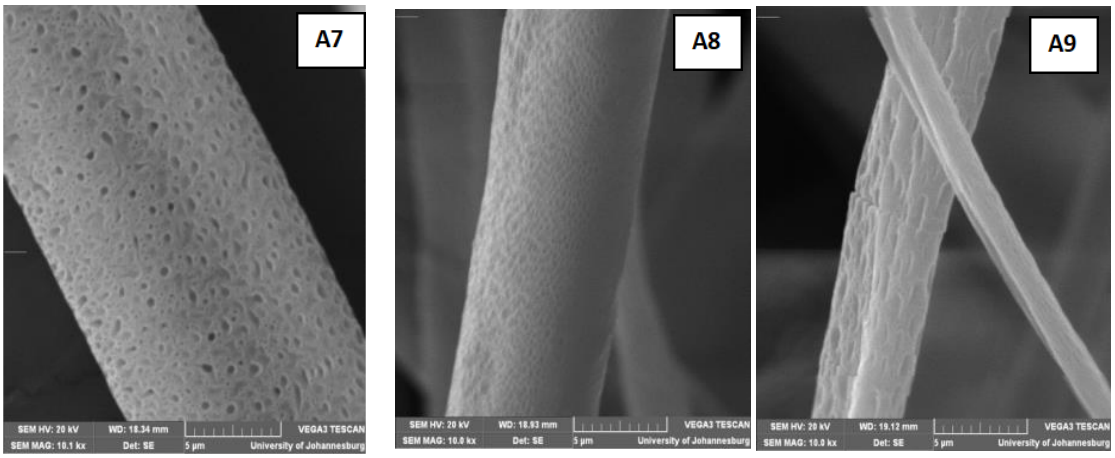

Figure 3: Micrograph of 20% EPS at [A7] 8.5 kV, [A8] 11.25 kV, [A9] 13.5 kV

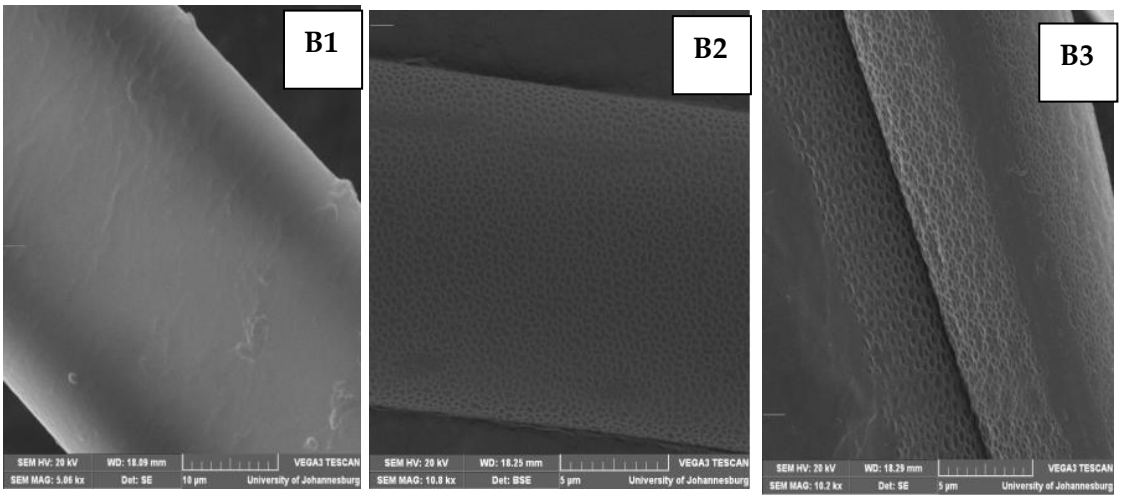

Figure 4: Micrograph of 30% EPS at [B1] 8.5 kV, [B2] 11.25 kV, [B3] 13.5 kV

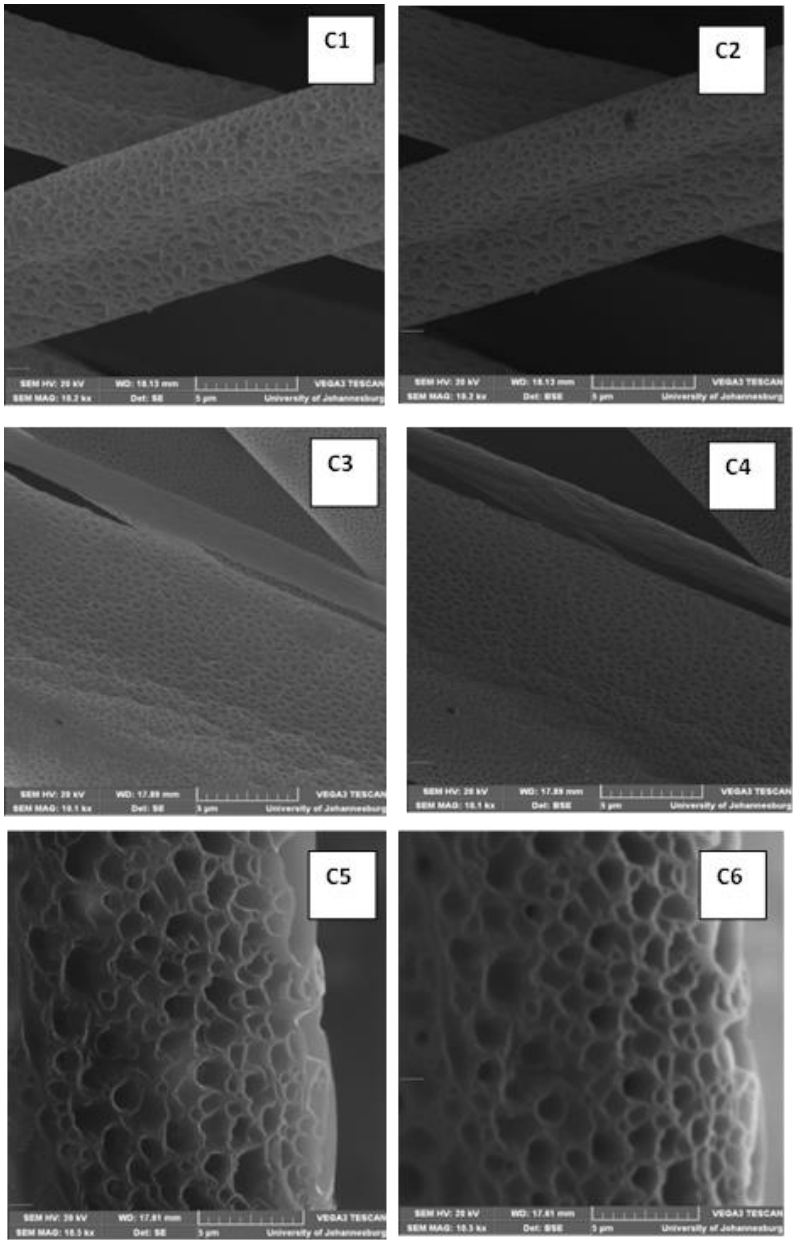

Figure 5: Micrograph of 20% EPS at 10kV [C1] SE, [C2] BSE; 15kV [C3] SE, [C4] BSE; 18.5kV [C5] SE, [C6] BSE.

Figures 6a-b show the BET Isotherm and pore distribution plots of beaded and porous (10 and 20% w/v respectively) EPS fibres. The adsorption-desorption isotherms of nitrogen gas on the solid surface of a membrane provide sufficient information essential for the in-depth understanding of adsorption equilibrium. Figure 6a shows the nitrogen adsorption-desorption of beaded fibre, isotherm can be categorized as type III according to the IUPAC classification of isotherm plots (Donohue & Aranovich 1998). However, Chakraborty *et al.* recently modified the IUPAC classification, based on this recently modified classification the isotherm remains type III (Chakraborty & Sun 2014). The pores distribution plot showed that micro-pores were dominantly used for the adsorption-desorption of the gas. During the gas adsorption-desorption process, the macro-pore was passive. Theoretical weak interaction predicted for this category of adsorbed could be based on the pore volume of micro-pores. Adsorption-desorption isotherm of beaded fibre was type III according to IUPAC and modified IUPAC classification (Chakraborty & Sun 2014; Donohue & Aranovich 1998). Also, meso and micropores were majorly utilized for adsorption-desorption of nitrogen gas. The presence of macro-pore is confirmed in porous and non-beaded fibre as seen in Figure 6b, which followed a similar trend in terms of isotherms classification. Though, the same in terms of isotherms classification, pore distribution curves confirmed a difference in pore orientation. Meso-pores prevailed in porous fibre with a trace population of micro-pores, this might be responsible for the enhancement in the volume of gas adsorbed. This alteration is a result of an increase in polymer concentration while the voltage was kept constant.

Furthermore, the variation in pore distribution resulted in adsorption average pore width of 71.22 to 70.10 nm for porous beaded fibre and porous fibre respectively. Comparison of these values with estimated SEM average pore width for the same fibres, beaded fibre: 150.25 nm; porous fibre: 127.50 nm. The SEM values were higher than BET average pore width, a difference may be due to an estimation of interior pores by BET Isotherms since it is based on gas adsorption. On the other hand, exterior pores on the fibre were estimated for SEM pores width.

4. Conclusion

The effect of polymer concentration on pore formation in electrospun fibre was established. This factor plays a crucial role to determine the rheological properties of the solution. Polymer migration is enabled due to the electrostatic force resulting in polymer and solvent rich phases. The solvent rich phase was favoured by a low concentration of solute thereby resulting in porous beaded fibre at various applied voltages. An increase in concentration vis-à-vis voltage favoured polymer-rich phase which is essential for porous fibre formation. This was supported by the co-existence of porous and non-porous fibre at high concentrations. Therefore, polymer concentration moderates variables interaction during chaotic motion in the electrospinning jet. The moderation results to phase separation which controls fibre orientation. Therefore, pore formation does not solely depend on long acclaimed principles TIPS, VIPS, and breath figure, it is also dependent on polymer concentration. Pore morphology examination using either SE or BSE was validated, either of the detectors can also be used for the examination of porous materials. Finally, the effect of the polymer-rich phase as a principle in the science of electrospun fibre is established. Another pathway for re-use of EPS is presented in membrane technology.

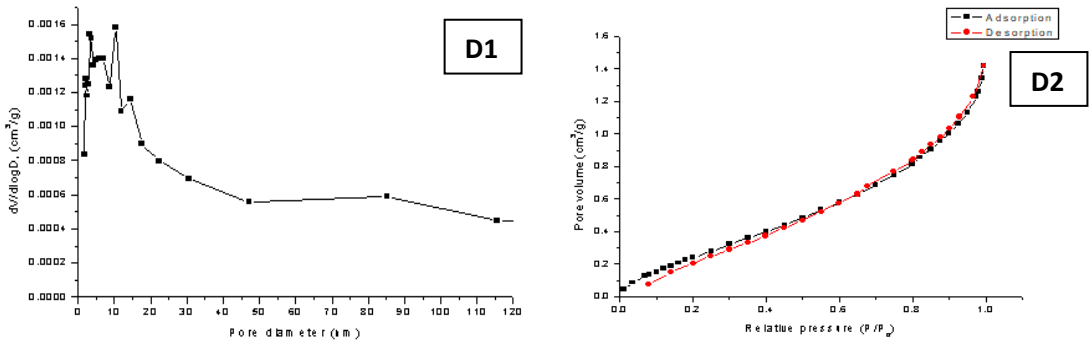

Figure 6a: Pore distribution (D1) and Nitrogen adsorption-desorption (D2) isotherms of beaded fibre

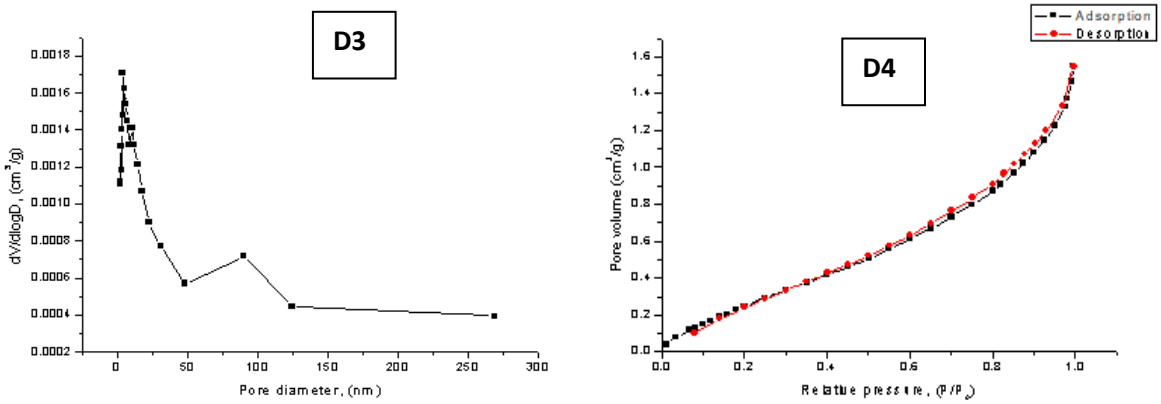

Figure 6b: Pore distribution (D3) and Nitrogen adsorption-desorption isotherms (D4) of porous fibre

Authors contribution

S.O. Alayande and J.N. Edokpayi conceptualized the idea with experimental works. O.A. Adeyemi and O. B. Akinsipo interpreted the experimental results. T. A.M. Msagati provided funding for the use of experimental facilities. All authors contributed to the manuscript development.

Conflict of interests

The authors declared no conflict of interest.

Authors' ORCID: Samson O. Alayande; ORCID: https://orcid.org/0000-0001-6309-8752
Oluseyi A. Adeyemi; ORCID: https://orcid.org/0000-0002-3992-5591
Oyesolape B. Akinsipo; ORCID: https://orcid.org/0000-0001-5531-112X
Joshua N. Edokpayi; ORCID: https://orcid.org/0000-0002-2550-3988
Titus A.M. Msagati; ORCID: https://orcid.org/0000-0002-9621-5051

References

Alayande, S. O., Dare, E. O., Akinlabi, A. K., Aiyedun, P. O., & Msagati, T. A. M. (2017). Novel electrospun superhydrophobic sorbent for petroleum fingerprinting analysis. *Polymer Bulletin*, 75:1, 75(1), 427–440. https://doi.org/10.1007/S00289-017-2036-9

Alayande, S. O., Dare, E. O., Msagati, T. A. M., Akinlabi, A. K., & Aiyedun, P. O. (2016a). Superhydrophobic and super oleophilic surface of porous beaded electrospun polystyrene and polystyrene-zeolite fibre for crude oil-water separation. *Physics and Chemistry of the Earth, Parts A/B/C*, 92, 7–13. https://doi.org/10.1016/J.PCE.2015.10.002

Alayande, S. O., Dare, E. O., Olorundare, F. O. G., Nkosi, D., Msagati, T. A. M., & Mamba, B. B. (2016b). Superoleophillic electrospun polystyrene/exfoliated graphite fibre for selective removal of crude oil from water. *Physics and Chemistry of the Earth, Parts A/B/C*, 92, 3–6. https://doi.org/10.1016/J.PCE.2015.09.004

Alayande, S. O., Hlengilizwe, N., Dare, E. O., Msagati, T. A. M., Akinlabi, A. K., & Aiyedun, P. O. (2016c). Novel nanoporous sorbent for solid-phase extraction in petroleum fingerprinting. *Applied Physics A*, 122(4), 1–7. https://doi.org/10.1007/S00339-016-9931-Z

Aljabri, N. M., Lai, Z., Hadjichristidis, N., & Huang, K. W. (2017). Renewable aromatics from the degradation of polystyrene under mild conditions. *Journal of Saudi Chemical Society*, 21(8), 983–989. https://doi.org/10.1016/J.JSCS.2017.05.005

Aziz, S. B., Hussein, G., Brza, M. A., Mohammed, S. J., Abdulwahid, R. T., Saeed, S. R., & Hassanzadeh, A. (2019). Fabrication of interconnected plasmonic spherical silver nanoparticles with enhanced localized surface

plasmon resonance (LSPR) peaks using quince leaf extract solution. *Nanomaterials*, 9(11), 1557. https://doi.org/10.3390/NANO9111557

Chakraborty, A., & Sun, B. (2014). An adsorption isotherm equation for multi-type adsorption with thermodynamic correctness. *Applied Thermal Engineering*, 72(2), 190–199. https://doi.org/10.1016/J.APPLTHERMALENG.2014.04.024

de Farias, L. M. S., Ghislandi, M. G., de Aguiar, M. F., Silva, D. B. R. S., Leal, A. N. R., de A.O. Silva, F., … Alves, K. G. B. (2022). Electrospun polystyrene/graphene oxide fibres are applied to the remediation of dye wastewater. *Materials Chemistry and Physics*, 276, 125356. https://doi.org/10.1016/J.MATCHEMPHYS.2021.125356

Ding, B., & Yu, J. (Eds.). (2014). *Electrospun Nanofibers for Energy and Environmental Applications*. https://doi.org/10.1007/978-3-642-54160-5

Donohue, M. D., & Aranovich, G. L. (1998). Classification of Gibbs adsorption isotherms. *Advances in Colloid and Interface Science*, 76–77, 137–152. https://doi.org/10.1016/S0001-8686(98)00044-X

Haller, P. D., Bradley, L. C., & Gupta, M. (2013). Effect of surface tension, viscosity, and process conditions on polymer morphology deposited at the liquid-vapour interface. *Langmuir*, 29(37), 11640–11645. https://doi.org/10.1021/LA402538E

Hidalgo-Crespo, J., Soto, M., Amaya-Rivas, J. L., & Santos-Méndez, M. (2022). Carbon and water footprint for the recycling process of expanded polystyrene (EPS) post-consumer waste. *Procedia CIRP*, 105, 452–457. https://doi.org/10.1016/J.PROCIR.2022.02.075

Jalali Alenjareghi, M., Rashidi, A., Kazemi, A., & Talebi, A. (2021). Highly efficient and recyclable spongy nanoporous graphene for remediation of organic pollutants. *Process Safety and Environmental Protection*, 148, 313–322. https://doi.org/10.1016/J.PSEP.2020.09.054

Knapczyk-Korczak, J., Zhu, J., Ura, D. P., Szewczyk, P. K., Gruszczyński, A., Benker, L., … Stachewicz, U. (2021). Enhanced Water Harvesting System and Mechanical Performance from Janus Fibers with Polystyrene and Cellulose Acetate. *ACS Sustainable Chemistry and Engineering*, 9(1), 180–188. https://doi.org/10.1021/ACSSUSCHEMENG.0C06480/SUPPL_FILE/SC0C06480_SI_001.PDF

Lu, P., Huang, Q., Mukherjee, A., & Hsieh, Y. Lo. (2011). Effects of polymer matrices on the formation of silicon carbide (SiC) nanoporous fibres and nanowires under carbothermal reduction. *Journal of Materials Chemistry*, 21(4), 1005–1012. https://doi.org/10.1039/C0JM02543G

Mirjalili, M., & Zohoori, • Salar. (2016). Review for application of electrospinning and electrospun nanofibers technology in the textile industry. *Journal of Nanostructure in Chemistry*, 6(3), 207–213. https://doi.org/10.1007/S40097-016-0189-Y

Oluwagbemiga Alayande. (2012). Porous and non-porous electrospun fibres from discarded expanded polystyrene. *International Journal of the Physical Sciences*, 7(11). https://doi.org/10.5897/IJPS11.1783

Pierini, F., Lanzi, M., Nakielski, P., & Kowalewski, T. A. (2017). Electrospun Polyaniline-Based Composite Nanofibers: Tuning the Electrical Conductivity by Tailoring the Structure of Thiol-Protected Metal Nanoparticles. *Journal of Nanomaterials*, 2017, 6142140. https://doi.org/10.1155/2017/6142140

Rudisill, S. G., Wang, Z., & Stein, A. (2012). Maintaining the structure of templated porous materials for reactive and high-temperature applications. *Langmuir*, 28(19), 7310–7324. https://doi.org/10.1021/LA300517G

Shepa, I., Mudra, E., & Dusza, J. (2021). Electrospinning through the prism of time. *Materials Today Chemistry*, 21, 100543. https://doi.org/10.1016/J.MTCHEM.2021.100543

SIMHA, R. (1949). Effect of concentration on the viscosity of dilute solutions. *Journal of Research of the National Bureau of Standards*, 42(4), 409–418. https://doi.org/10.6028/JRES.042.036

ŞİMŞEK, M. (2019). Altering Surface Topography of Electrospun Fibers. *Natural and Applied Sciences Journal*, 2(1), 8–14. https://doi.org/10.38061/IDUNAS.569788

Szewczyk, P. K., & Stachewicz, U. (2020). The impact of relative humidity on electrospun polymer fibres: From structural changes to fibre morphology. *Advances in Colloid and Interface Science*, 286, 102315. https://doi.org/10.1016/J.CIS.2020.102315

Uttaravalli, A. N., Dinda, S., & Gidla, B. R. (2020). Scientific and engineering aspects of potential applications of post-consumer (waste) expanded polystyrene: A review. *Process Safety and Environmental Protection*, 137, 140–148. https://doi.org/10.1016/J.PSEP.2020.02.023

Xie, W., Li, J., Sun, F., & Dong, W. (2020). Ultrasonication favours TiO_2 nano-particle dispersion in PVDF ultrafiltration membrane to effectively enhance membrane hydrophilicity and anti-fouling capability. *Environmental Science and Pollution Research*, 27(9), 9503–9519. https://doi.org/10.1007/S11356-019-06862-9

Xue, J., Wu, T., Dai, Y., & Xia, Y. (2019). Electrospinning and electrospun nanofibers: methods, materials, and applications. *Chemical Reviews*, 119(8), 5298–5415. https://doi.org/10.1021/ACS.CHEMREV.8B00593

Xue, J., Xie, J., Liu, W., & Xia, Y. (2017). Electrospun nanofibers: new concepts, materials, and applications. *Accounts of Chemical Research*, 50(8), 1976–1987. https://doi.org/10.1021/ACS.ACCOUNTS.7B00218

Yadav, C., Saini, A., & Maji, P. K. (2018). Cellulose nanofibres as biomaterial for nano-reinforcement of poly[styrene-(ethylene-co-butylene)-styrene] triblock copolymer. *Cellulose*, 25(1), 449–461. https://doi.org/10.1007/S10570-017-1567-4

Zhang, J.-H., Zhou, Z., Li, J., Shen, B., Zhu, T., Gao, X., … Pan, L. (2022). Coupling enhanced performance of triboelectric–piezoelectric hybrid nanogenerator based on nanoporous film of poly(vinylidene fluoride)/batio 3 composite electrospun fibers. *ACS Materials Letters*, 847–852. https://doi.org/10.1021/acsmaterialslett.1c00819